

# Role of Adenine Nucleotide Translocator 1 in mtDNA Maintenance

Jyrki Kaukonen,<sup>1</sup> Jukka K. Juselius,<sup>2\*</sup> Valeria Tiranti,<sup>3\*</sup> Aija Kytälä,<sup>1</sup> Massimo Zeviani,<sup>3</sup> Giacomo P. Comi,<sup>4</sup> Sirkka Keränen,<sup>2</sup> Leena Peltonen,<sup>1,5</sup> Anu Suomalainen<sup>1†</sup>

Autosomal dominant progressive external ophthalmoplegia is a rare human disease that shows a Mendelian inheritance pattern, but is characterized by large-scale mitochondrial DNA (mtDNA) deletions. We have identified two heterozygous missense mutations in the nuclear gene encoding the heart/skeletal muscle isoform of the adenine nucleotide translocator (*ANT1*) in five families and one sporadic patient. The familial mutation substitutes a proline for a highly conserved alanine at position 114 in the ANT1 protein. The analogous mutation in yeast caused a respiratory defect. These results indicate that ANT has a role in mtDNA maintenance and that a mitochondrial disease can be caused by a dominant mechanism.

Mitochondrial dysfunction caused by instability of mtDNA (depletion or multiple deletions) has been associated with a variety of inherited diseases, as well as with aging and exposure to the antiviral drug zidovudine (AZT) (1). Studies of an interesting subgroup of human mitochondrial disorders have revealed that nuclear mutations can affect the mtDNA copy number or its integrity. These diseases include mtDNA depletion syndrome (2), mitochondrial neurogastrointestinal encephalomyopathy (MNGIE) (3), and recessive and dominant forms of progressive external ophthalmoplegia with multiple deletions of mtDNA (4, 5).

Autosomal dominant progressive external ophthalmoplegia (adPEO) with multiple mtDNA deletions is an adult-onset mitochondrial disorder with an incidence of ~1:100,000 in Finland and in Italy. The typical clinical features are progressive external ophthalmoplegia, ptosis, and exercise intolerance. Ataxia, depression, hypogonadism, hearing deficit, peripheral neuropathy, and cataract are found in some families (5–8). The skeletal muscle shows ragged-red fibers and mildly reduced activities of the respiratory-chain enzymes, as well as multiple mtDNA deletions (Fig. 1).

There are three distinct autosomal loci for this disorder on chromosomes 10q24 (MIM 157640) (9), 3p14-21 (MIM 601226) (10), and 4q34-35 (MIM 601227) (11).

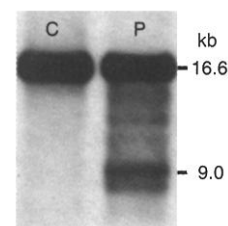
The critical region of the 4q-adPEO locus includes the gene encoding the heart- and skeletal muscle-specific isoform of the adenine nucleotide translocator (*ANT1*). ANT, or the ADP/ATP translocator, is the most abundant protein in the inner mitochondrial membrane (12). It forms as a homodimer, a gated channel by which ADP is brought into and ATP brought out of the mitochondrial matrix. ANT regulates the adenine nucleotide concentrations in the cytoplasm and within the mitochondria and mediates signals of nucleocytoplasmic energy consumption to the mitochondrial respiratory chain. In addition to the translocase activity, ANT is a core structural element of the mitochondrial permeability transition pore (MPTP) (13) and has an important role in mitochondrial-mediated apoptosis (14). Human ANT exists as three isoforms: ANT1 is expressed predominantly in postmitotic cell types in skeletal muscle, heart, and brain; ANT2 is expressed mainly in proliferating tissue types; and ANT3 is expressed ubiquitously (15, 16).

We analyzed the genomic sequence of *ANT1* in the 4q-linked Italian family A (Fig. 2) (17) and identified a heterozygous G→C transversion in exon 2, codon 114, which produces an Ala→Pro substitution (Fig. 3A). The nucleotide change was present in all the affected family members, but not in 860 Finnish or 150 Italian control individuals. A114 and its flanking sequence are strictly conserved between species, and thus likely to be functionally significant (Fig. 3, B and C). Next we analyzed *ANT1* in patients and healthy subjects of all the PEO families of our study material, including those with pre-

vious linkage to other chromosomal loci or with unknown gene loci (Table 1). The heterozygous A114P change was present in four additional families (B to E), two of which, surprisingly, had been previously linked to the chromosome 3 locus (10). We constructed 13.5-cM-long haplotypes with DNA markers flanking the *ANT1* locus and identified a common disease haplotype with identical marker alleles, shared by patients in the three Italian families A, B, and C (Fig. 2). This suggests that there is one founder mutation and common ancestry (Fig. 2), although this could not be genealogically confirmed. The A114P mutation segregated with the disease in all these families, with the exception of subject A/402 (Fig. 2). In one sporadic patient with PEO and multiple mtDNA deletions, we identified another missense mutation, a G→A transition in exon 4, codon 289, which produces a Val→Met substitution (Fig. 3, A and C, and Table 1). This sequence change was not present in the patient's clinically healthy parents [paternity tested (18)] or in 156 Italian or 921 Finnish control subjects and was therefore considered a new mutation.

Because of the previous linkage of families B and C to the chromosome 3 locus (10), we confirmed the clinical information on the family members. Upon reexamination, subject B/308 was found to be healthy, although he had been previously recorded as an adPEO patient. Family C was small, and its informativity in the linkage calculations was low. After updating of the phenotypic information, the analyses of the pedigree data with DNA markers from 3p14-21 failed to show significant lod (logarithm of the odds ratio for linkage) scores in this region (highest new multipoint lod score, 2.85) (19). Further, haplotype analyses did not support the existence of an adPEO locus on chromosome 3. These data emphasize the importance of accurate clinical diagnoses in restricted study samples.

**Fig 1.** Multiple mtDNA deletions in adPEO patient muscle. Total muscle DNA from a control subject (C) and an adPEO patient (P, patient from family C, Fig. 2) was digested with Pvu II, which linearizes the circular mtDNA. Southern blot analysis was done as described (5), with total human mtDNA as the hybridization probe. The 16.6-kb band indicates the full-size mtDNA, and the additional bands on the patient's sample represent the mutant mtDNA molecules with multiple deletions of different sizes. The amount of mutant mtDNA is about 50% of total mtDNA. MtDNA hybridization signal on each lane was compared with that of a nuclear 18S rDNA sequence by densitometry, and no sign of reduced total mtDNA was detected (39).



<sup>1</sup>National Public Health Institute, Department of Human Molecular Genetics, Mannerheimintie 166, 00300 Helsinki, Finland. <sup>2</sup>VTT Biotechnology, Espoo, Finland. <sup>3</sup>Division of Biochemistry and Genetics, Department of Neurological Research, National Neurological Institute "C. Besta," Milan, Italy. <sup>4</sup>Centro Dino Ferrari, Istituto di Clinica Neurologica, Università degli Studi di Milano, Istituto di Ricovero e Cura a Carattere Scientifico Ospedale Maggiore Policlinico, Milan, Italy. <sup>5</sup>Department of Human Genetics, University of California School of Medicine, Los Angeles, CA 10095-7088, USA.

\*These authors contributed equally to this work.

†To whom correspondence should be addressed. E-mail: anu@ericpc.mni.mcgill.ca

## REPORTS

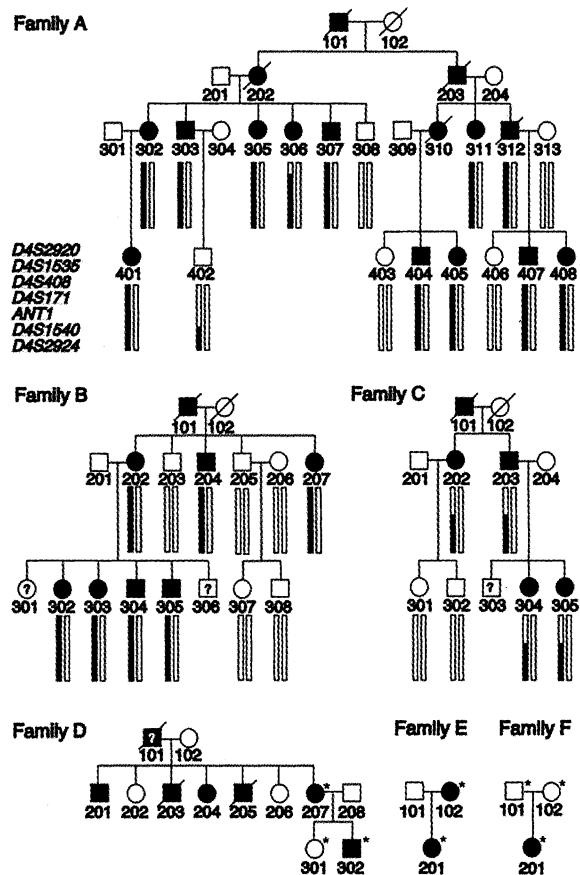
Human cells could not be used to evaluate functional consequences of the *ANT1* mutation. No disease phenotype has been identified in cultured cells of adPEO patients (20, 21); *ANT1* is not expressed in cultured cells, even in myoblasts (20); and apoptosis is induced when wild-type *ANT1* is overexpressed (22). Therefore, we introduced the A114→Pro mutation into the fully conserved site (A128) (Fig. 3C) of the major adenine nucleotide translocator *AAC2* gene of the yeast *Saccharomyces cerevisiae*. We transformed two different yeast strains lacking functional *AAC2* with constructs encoding wild-type *AAC2* or mutant *AAC2*, or with the single-copy vector only (23). On glucose medium, all the transformants grew equally well, because the anaerobic energy production is not dependent on *AAC2* function (Fig. 4A). On glycerol medium, the cells use the respiratory chain for energy production, and the mutant A128P transformants showed defective growth, as did the vector-only control, whereas the wild-type *AAC2* transformants formed single colonies with equal efficiency as on glucose medium (Fig. 4, A and B). This finding indicates that the A128P mutation on *AAC2*, corresponding to the A114P mutation in human *ANT1*, affects oxidative respiration. Analysis of the mtDNA in the mutant A128P transformants showed neither large-scale rearrangements nor depletion, suggesting that the growth defect is caused by an ADP/ATP transport defect (24) (Fig. 4C).

On the basis of the structural modeling of the yeast *AAC2*, A114P is likely to be located either in the third transmembrane domain of *ANT1* (25, 26), or just adjacent to it, in the loop joining the second and third transmembrane domains in the intermembrane space (27). The V289M mutation affects the sixth transmembrane domain (25–27). A simulation analysis of the secondary structure of human *ANT1* suggests that the A→P substitution at position 114 may cause an additional bend in the polypeptide, disrupting the local  $\alpha$  helix (28). The V289M mutation is also predicted to modify the  $\alpha$  helix. Because patients with dominant PEO carry one wild-type and one mutant allele, defective *ANT1* dimers would form in two out of three dimerization events.

No defects of the *ANT1* gene have previously been reported in humans, although *ANT1* deficiency and reduced transcript levels have been described in a patient with lactic acidosis and myopathy (29). Mice with targeted inactivation of *ANT1* show exercise intolerance mimicking mitochondrial myopathy, as well as hypertrophic cardiomyopathy (30). The muscle in these mice exhibits dramatic proliferation of mitochondria and reduced rates of mitochondrial ADP-stimulated respiration (30), and both muscle and heart DNA exhibit multiple deletions of mtDNA (31). Although the dominant

mutation in humans differs from the gene inactivation in mice, the disease phenotypes are similar, except that humans do not have cardiac symptoms.

**Fig. 2.** AdPEO pedigrees and shared chromosomal regions on 4q34–35. We have previously described the clinical features of families A (11) as well as B and C (10). The common manifestation of the disease was chronic progressive external ophthalmoplegia, and the age of onset for the symptoms was <45 years. The neuromuscular symptoms were largely confined to eye and facial muscles in families A, C, D, and F, whereas patients from families B and E also had generalized muscle weakness. Peripheral neuropathy, endocrinological abnormalities, or symptoms from the central nervous system, described in some adPEO families (5–8), were not present. Families A to E originate from Romagna County of Italy, suggesting that there may be common ancestry and one founder mutation. Informed consent was obtained from all family members, and total DNA was extracted from lymphoblasts, cultured fibroblasts, or 10 to 150 mg of muscle biopsy sample (40). The individuals with distinct clinical symptoms and/or deletions of mtDNA, detected by Southern blot hybridization, are indicated with black symbols. The white symbols indicate clinically investigated individuals of age >45 years with no clinical symptoms. The individuals marked with question marks have not been clinically investigated or are <45 years old. Haplotypes of chromosome 4q34–35 adPEO region were constructed as described (11), with the indicated 4q DNA markers. The allelically identical part of the haplotype, and consequently the segregation of the A114P mutation, is indicated with a black bar. In families D to F the individuals of whom DNA samples were available are marked with an asterisk. The A114P mutation segregated with the disease in families A to E, with the exception of subject A/402, an asymptomatic carrier of the *ANT1* mutation (49 years). Because this subject's muscle sample was not available, his disease status could not be determined. The only patient in family F had the V289M mutation.



Our results suggest that in yeast the A128P mutation disrupts ADP/ATP translocation, because no acute instability of mtDNA was detected. However, in humans

**Table 1.** PEO family and patient material and controls analyzed for *ANT1* mutations. We analyzed *ANT1* for the presence of the A114P and V289M mutations in Italian adPEO families, in adPEO and recessive PEO (arPEO) families from other European countries or the United States, and in sporadic Italian PEO patients with multiple mtDNA deletions. Control samples were Italian or Finnish, either analyzed individually or from pooled samples of Finnish control subjects. Samples were analyzed by PCR and subsequent sequencing or solid-phase minisequencing (37). The detected genotypes were as follows: AA, alanine/alanine; AP, alanine/proline at amino acid position 114; VV, valine/valine; and VM valine/methionine at amino acid position 289 of *ANT1*.

ANT1 amino acid	Nationality	AdPEO families (n)		Sporadic PEO patients (n)		ArPEO families (n)	Control subjects (n)
		AA	AP	AA	AP		
114	Italian	29	5	13	0	0	150
	Other	7	0	0	0	2	860
289	Italian	34	0	12	1	0	156
	Other	7	0	0	0	2	921

## REPORTS

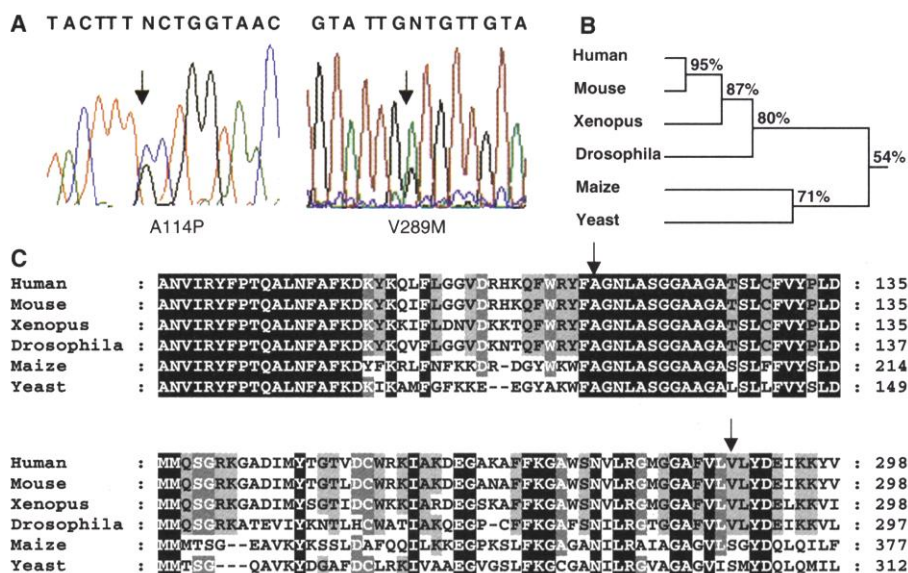


**Fig. 3.** The heterozygous A114P and V289M mutations and sequence conservation of ANT1. (A) DNA sequence around codon 114 (left) and 289 (right) in two patients. The heterozygous G→C and G→A missense mutations are marked with arrows. (B) Conservation of ANT1/AAC2 amino acid sequence in different species. The mouse ANT1 is 95% identical and AAC2 is 54% identical with human ANT1. (C) A114 of ANT1 (arrow) is highly conserved, and V289 (arrow) relatively conserved between species. The sequence between amino acids 113 and 125 of ANT1 is fully conserved in AAC2, the *S. cerevisiae* homolog of ANT1. Abbreviations for the amino acid residues are as follows: A, Ala; C, Cys; D, Asp; E, Glu; F, Phe; G, Gly; H, His; I, Ile; K, Lys; L, Leu; M, Met; N, Asn; P, Pro; Q, Gln; R, Arg; S, Ser; T, Thr; V, Val; W, Trp; and Y, Tyr.

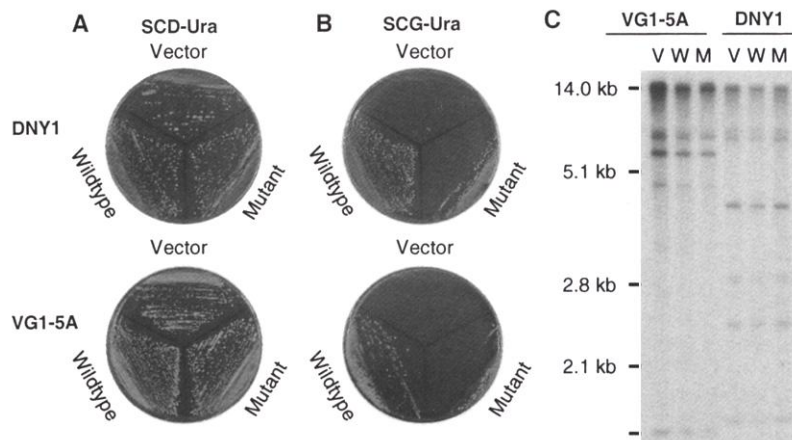


**Fig. 4.** Functional consequences of the A128P mutation of AAC2, *S. cerevisiae* homolog of ANT1. The *S. cerevisiae* haploid yeast strains were as follows: DNY1 (*MATa aac1::LEU2 aac2::HIS3 his3-11,15 trp1-1 ura3-1 can1-100 ade2-1 leu2-3,112*) (27), and VG1-5A (*MATα ade ura3 trp1 op1*) (41). DNY1 is an *aac1 aac2* double-deletion strain, and strain VG1-5A has an *op1* mutation in AAC2 gene, both resulting in lack of growth in nonfermentable carbon sources. The aerobic growth defect caused by the double mutation is similar to that of *aac2* mutant only (42). (A) Growth in glucose medium (SCD-Ura) when strains were transformed with vector control (pSEYc58) wild-type AAC2 (pSEYc58AAC2) or the mutant AAC2 (pSEYc58aac2<sup>A128P</sup>) construct. All the transformants grew equally well. (B) Growth on glycerol medium (SCG-Ura). Strains transformed with vector control were unable to grow on glycerol, and those expressing the mutant AAC2 showed a clear defect in growth on glycerol compared with the transformants expressing the wild-type AAC2. The growth of the transformants was tested also as patches first grown on glucose and then replicated onto glycerol. A distinct growth defect was observed for the AAC2<sup>A128P</sup> mutant compared with the wild-type allele (43). The difference in growth efficiency on glycerol was apparent on the first day after replication. On the second day the mutant cells started to grow, but the difference in growth rate was still observed. In transformation of a haploid wild-type yeast strain with a single-copy AAC2 mutant plasmid, we could not detect a growth defect (43). (C) MtDNA analysis of vector (V), wild-type AAC2 (W), and mutant AAC2 (M) transformants. Southern hybridization analysis of Acc I restriction-digested DNA was carried out with a yeast mtDNA-specific oligonucleotide as a probe (24). MtDNA on each lane was quantified by densitometry using the hybridization signal of a single-copy nuclear gene, MSO1, as an internal control (43). Neither large-scale rearrangements nor depletion of mtDNA in the mutant AAC2 transformants was detected.

the ANT1 defect causes secondary accumulation of mtDNA mutations in postmitotic cells by a still unknown mechanism. A defect in the cytoplasmic thymidine phosphorylase in MNGIE syndrome with multiple mtDNA deletions suggests that disturbed intramitochondrial deoxynucleoside triphosphate (dNTP) pools may have a role in mtDNA deletion formation (32), possibly by increasing the error rate of the mitochondrial  $\gamma$ -polymerase. In postmitotic cells, the short mutant mtDNA may have a replicative advantage over the wild-type mtDNA, possibly resulting in accumulation of mutant mtDNA. Current knowledge does not support dATP as a physiological substrate for ANT (12). However, mammalian mitochondria contain enzymes required to reduce ADP to form dADP, which is phosphorylated to form dATP for DNA synthesis (33, 34), so it is conceivable that ANT regulates intramitochondrial dATP concentrations. Several additional mechanisms may modify the adPEO pathogenesis caused by ANT1 defect: (i) the structural defect in ANT1 may affect MPTP opening; (ii) misfolding of ANT1 may expose the protein to oxidative lesions and cause its premature age-related inactivation (35); and/or (iii) dysfunction of ANT1 may increase oxidative stress within mitochondria (31).

The mutant mtDNA is likely to participate in the pathogenesis of adPEO. The proportion of mutant mtDNA in patients increases slowly with age and follows the disease severity (8). In addition, the progression, symptoms, and mutant mtDNA amount of adPEO resemble closely those associated with sporadic PEO with single mtDNA deletions, a disease known to be caused by the mutant mtDNA.

Finally, it is of interest that adPEO is mediated by a dominant mechanism, in contrast to other mitochondrial disorders due to nuclear gene defects, which are caused by loss-of-function mutations. Our finding may provide new insight into the pathogenesis of mitochondrial disorders and form the basis for future studies on mtDNA stability and the function of ANT.

### References and Notes

1. A. Suomalainen, *Ann. Med.* **29**, 235 (1997).
2. C. T. Moraes et al., *Am. J. Hum. Genet.* **48**, 492 (1991).
3. M. Hirano et al., *Neurology* **44**, 721 (1994).
4. S. Bohlega et al., *Neurology* **46**, 1329 (1996).
5. M. Zeviani et al., *Nature* **339**, 309 (1989).
6. S. Servidei et al., *Neurology* **41**, 1053 (1991).
7. A. Melberg, P. O. Lundberg, K. G., Henriksson, Y. Olsson, E. Stalberg, *Muscle Nerve* **19**, 751 (1996).
8. A. Suomalainen et al., *Neurology* **48**, 1244 (1997).
9. A. Suomalainen et al., *Nature Genet.* **9**, 146 (1995).
10. J. A. Kaukonen et al., *Am. J. Hum. Genet.* **58**, 763 (1996).
11. J. Kaukonen et al., *Am. J. Hum. Genet.* **65**, 256 (1999).
12. M. Klingenberg, in *The Enzymes of Biological Membranes: Membrane Transport*, A. N. Martinosi, Ed. (Plenum, New York and London, 1976), vol. 3, pp. 383-438.

13. N. Brustovetsky and M. Klingenberg, *Biochemistry* **35**, 8483 (1996).
14. I. Marzo *et al.*, *Science* **281**, 2027 (1998).
15. G. Stepien, A. Torroni, A. B. Chung, J. A. Hodge, D. C. Wallace, *J. Biol. Chem.* **267**, 14592 (1992).
16. A. Doerner *et al.*, *FEBS Lett.* **414**, 258 (1997).
17. To amplify the coding region of human *ANT1* (GenBank accession number, J04982), we designed primers from intronic sequences flanking the following exons: exon 1, 1F (5'-GCTCGGCCGGACAGATAACA-TGAAT) and 1R (5'-TGGCATAAGACGGTGCCAAA-AATA); exon 2, 2F (5'-AATCTAGGAAGTGCAAACC) and 2R (5'-TGTGAGTTATAGATCCCATATA); exon 3, 3F (5'-GCAAGGTCAGAGCATGGA) and 3R (5'-TGTA-AAATGTTCTCTCGG); exon 4, 4F (5'-ATGCCCA-GATGACCCTGATT) and 4R (5'-AACCCACAATG-GATCTGTG). Polymerase chain reaction (PCR) amplification was carried out in a volume of 50  $\mu$ l containing 50 ng of genomic DNA, 0.2  $\mu$ M of each primer plus 200  $\mu$ M of each dNTP, and 1.25 U of DNA polymerase (DynaZyme, Finnzymes, Finland). Cycling conditions were as follows: 95°C for 30 s, 56°C for 30 s, and 72°C for 45 s; 33 cycles, with an initial 3-min denaturation at 95°C and a final 10-min extension at 72°C. To amplify exon 1, we included 1 M betaine (Sigma). DNA sequence was analyzed by PCR-cycle sequencing and visualized by 377 ABI Sequencer (Applied Biosystems, Foster City, CA).
18. M. Zeviani, data not shown.
19. Haplotype construction and linkage calculations of the chromosome 3 adPEO region marker data with the updated clinical information were done as described (10).
20. A. Suomalainen and M. Zeviani, unpublished data.
21. R. Carozzo, M. M. Davidson, W. F. Walker, M. Hirano, A. F. Miranda, *J. Neurol. Sci.* **170**, 24 (1999).
22. M. K. A. Bauer, A. Schubert, O. Rocks, S. Grimm, *J. Cell Biol.* **147**, 1493 (1999).
23. Yeast cells were grown at 30°C in YPD (1% yeast extract, 2% peptone, 2% glucose) or in synthetic complete medium, with 2% glucose (SCD) or 2% glycerol (SCG) as the carbon source, respectively. Yeast transformants were selected on SCD-Ura and tested for growth on SCG-Ura (36). The single-copy AAC2 expression vector, pSEYc58AAC2 (27), was a *CEN-ARS URA3* plasmid encoding the wild-type AAC2 derived from genomic DNA of *S. cerevisiae* (GenBank accession number J04021). The vector control, pSEYc58, was obtained by removing the AAC2 fragment from pSEYc58AAC2 by Pvu II digestion. For the mutagenesis, the AAC2 fragment from pSEYc58AAC2 was released and inserted into pGEM-4Z (Promega) to obtain pGEMAAC2. Mutagenesis was carried out with the Chameleon kit (Stratagene). The mutagenesis primer introduced the analogous Ala $\rightarrow$ Pro substitution to AAC2 (amino acid 128), as in human ANT1 (amino acid 114). Screening of the mutant colonies was carried out by PCR and solid-phase minisequencing (37). The mutant pGEMAAC2 insert was released and inserted back into pSEYc58 to obtain pSEYc58aac2<sup>A128P</sup>. The correct orientation and sequence of the insert were confirmed by DNA sequencing.
24. Yeast total genomic DNA was extracted by standard methods and digested with Acc I (New England Biolabs, Herts, UK). The concentration of DNA in the samples was determined spectrophotometrically after the digestion to confirm loading of equal amounts of DNA (3  $\mu$ g). Southern hybridization analysis was carried out by standard methods, with a 5'-[ $\gamma$ -<sup>32</sup>P]ATP end-labeled yeast mtDNA-specific sequence repeat (5'-CTCCTTCGGGGTTCGGCTCCCGTGG CCGGG CCGGG-3') as a hybridization probe.
25. J. E. Walker and M. J. Runswick, *J. Bioenerg. Biomembr.* **25**, 435 (1993).
26. V. Müller, G. Basset, D. R. Nelson, M. Klingenberg, *Biochemistry* **35**, 16132 (1996).
27. D. R. Nelson, J. E. Lawson, M. Klingenberg, M. G. Douglas, *J. Mol. Biol.* **230**, 1159 (1993).
28. All of the proteins used for sequence comparison were retrieved from SWISS-PROT by Entrez query. Version 1.8 of ClustalW at European Bioinformatics Institute (<http://www2.ebi.ac.uk/clustalw/>) with default parameters was used for multiple sequence alignment, and DNAMAN software (Lynnon Biosoft) for graphical enhancement. The secondary-structure predictions were carried out with the PHDsec program (38).
29. H. D. Bakker *et al.*, *J. Inher. Metab. Dis.* **16**, 548 (1993).
30. B. H. Graham *et al.*, *Nature Genet.* **16**, 226 (1997).
31. L. A. Esposito, S. Melov, A. Panov, B. A. Cottrell, D. C. Wallace, *Proc. Natl. Acad. Sci. U.S.A.* **96**, 4820 (1999).
32. I. Nishino, A. Spinazzola, M. Hirano, *Science* **283**, 689 (1999).
33. J. Bodenstern-Lang, A. Buch, Follmann H. *FEBS Lett.* **258**, 22 (1989).
34. P. Young, J. M. Leeds, M. B. Slabaugh, C. K. Mathews, *Biochem. Biophys. Res. Commun.* **203**, 46 (1994).
35. L. J. Yan, R. S. Sohal, *Proc. Natl. Acad. Sci. U.S.A.* **95**, 12896 (1998).
36. J. Toikkanen *et al.*, *Yeast* **12**, 425 (1996).
37. A.-C. Syvänen, *Clin. Chim. Acta.* **226**, 225 (1994).
38. B. Rost and C. Sander, *Proteins* **19**, 55 (1994).
39. V. Tiranti, data not shown.
40. M. Zeviani *et al.*, *Neurology* **38**, 1339 (1988).
41. A. M. Viola, C. L. Galeotti, P. Goffrini, A. Ficarelli, I. A. Ferrero, *Curr. Genet.* **27**, 229 (1995).
42. T. Drgon, L. Sabova, G. Gavurnikova, J. Kolarov, *FEBS Lett.* **304**, 277 (1992).
43. J. Juselius and S. Keränen, data not shown.
44. We thank T. Fox for pSEYc58AAC2 and advice, D. Nelson for strain DNY1, and A. M. Viola for VG1-5A strain; G. Galassi, M. G. Piscaglia, and F. Salvi for clinical characterization of patients; E. Shoubridge and K. Wartiovaara for helpful discussions; and R. Timonen, P. Tainola, F. Carrara, and A. Bordoni for technical assistance. Supported by grants from the Maud Kuistila Memorial Foundation, Oskar Öflund Foundation, and Finnish Medical Foundation (J.K.); Telethon-Italy (grant 1180), Ministero della Sanita (030.3/RF98.37), and European Union Human Capital and Mobility on "mitochondrial biogenesis in development and disease" (M.Z.); the Academy of Finland grant 42160 (S.K.); the Emil Aaltonen Foundation (A.S.); and Helsinki Graduate School in Biotechnology and Molecular Biology (J.J.).

14 February 2000; accepted 16 June 2000

# Involvement of Cellular Caveolae in Bacterial Entry into Mast Cells

Jeoung-Sook Shin, Zhimin Gao, Soman N. Abraham\*

Caveolae are subcellular structures implicated in the import and transcytosis of macromolecules and in transmembrane signaling. To date, evidence for the existence of caveolae in hematopoietic cells has been ambiguous. Caveolae were detected in the microvilli and intracellular vesicles of cultured mouse bone marrow-derived mast cells (BMMCs). CD48, a receptor for FimH-expressing (type 1 fimbriated) *Escherichia coli*, was specifically localized to plasmalemmal caveolae in BMMCs. The involvement of caveolae in bacterial entry into BMMCs was indicated because caveolae-disrupting and -usurping agents specifically blocked *E. coli* entry, and markers of caveolae were actively recruited to sites of bacterial entry. The formation of bacteria-encapsulating caveolar chambers in BMMCs represents a distinct mechanism of microbial entry into phagocytes.

Originally defined by their caveolike morphology (1), caveolae are pleomorphic membrane structures characterized biochemically by their buoyant density; resistance to nonionic detergents; and enrichment in cholesterol, glycolipids such as the glycosphingolipid G<sub>M1</sub>, and a specific protein, caveolin (2–4). Caveolae participate in the transcytosis of macromolecules across capillary endothelial cells (5) and in the concentration of small molecules internalized by potocytosis (6). They also serve as conduits for transmembrane signaling, containing high concentrations of signaling molecules (7, 8). Although believed to be present in virtually all cell types, the presence of caveolae in hematopoietic cells has not been clear. Cell lines of lymphocytes (9) and mast cells (10) appear to possess membrane domains consistent with caveolae but have not been shown to contain

caveolin. We investigated whether mouse BMMCs form caveolae. Mast cells play a crucial role in recruiting neutrophils to sites of bacterial infection (11, 12). They can also phagocytose a wide range of bacteria (13). In antibody-deficient conditions, however, these cells and other phagocytes support the entry and subsequent survival of FimH-expressing *E. coli* (14, 15).

Caveolar fractions were isolated from BMMCs (Fig. 1A). Immunogold microscopy of cross sections of BMMCs with caveolin-specific antibody labeled microvilli and intracellular vesicles (Fig. 1D). Thus, although BMMCs did not appear to form caveolae in their plasma membranes, vesicular and plasmalemmal forms of caveolae were present. The presence of glycosylphosphatidylinositol (GPI)-anchored molecules in native caveolae is controversial (16–18). We determined that CD48, a GPI-anchored molecule, was associated with caveolae of BMMCs (Fig. 1, A and C). Confocal microscopy of BMMCs revealed colocalization of CD48 with caveolin primarily in the plasma

Departments of Pathology and Microbiology, Duke University Medical Center, Durham, NC 27710, USA.

\*To whom correspondence should be addressed. E-mail: abrah006@mc.duke.edu